FINAL EXECUTIVE SUMMARY REPORT

Title of the Project: Pilot-scale Demonstration of Catalytic Wyoming Coal Gasification and

Syngas Processing (Diesel Production) Technologies

Maohong Fan

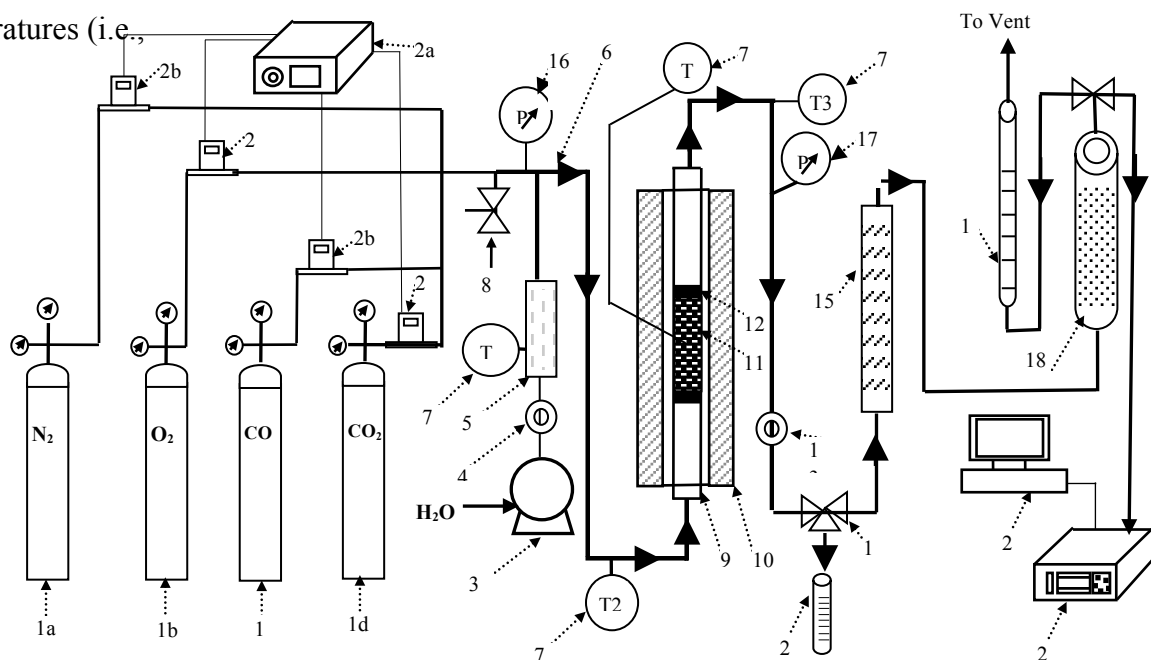**University of Wyoming**

6/30/2016

1.   ABSTRACT

The overall objective of the proposed project was to produce diesel with the manner of maximum economic benefit and minimum environmental impact, which was achieved by using innovative technologies and Wyoming resources including Wyoming coal and trona as well as rare earth elements. The project was designed to make progress in converting Wyoming coal to high-value fuel or chemicals. Upon the completion of the project, promising catalytic gasification, CO_2 separation and following significant results have been achieved.

2.   METHODS

2.1   Coal gasification

The catalytic gasification apparatus used in this research is shown in G-Figure 1. About 5.0 g dry-ash-free (DAF) coal was used for each gasification test. Initially, the coal sample was heated in N_2 with a flow rate of 4.1 ml/min at 20°C/min to the desired gasification temperature, followed by introducing steam at a flow rate of 0.04 g/min. The gasses used for conducting the catalytic gasification study are ultra-high-purity (UHP) N_2 (US Welding), O_2 (Air Liquide), CO (US Welding), and CO_2 (Praxair). The flow rates of the gasses were controlled using mass flowmeters as shown (2) in G-Figure 1 (Porter Instruments series 201 with a 4 channel PCIM4 controller). Water addition was realized by a high-pressure pump (3) (Scientific Systems-Lab

Alliance Series 1) with a back pressure regulator (4) (GO Regulator). The liquid water was

vaporized in a coil type vaporizer (5) surrounded with heating tape. The stainless steel tubing

before and after the ½" (13 mm) diameter tubular stainless steel tube reactor (9) was heat traced

(6), with the temperatures monitored by thermocouples (7), to preheat the gas/water vapor

mixture and to prevent coal tar and water from condensing at the reactor outlet. Additional

insulation was installed as needed in different sections of the piping throughout the system.

Ceramic wool (12) was inserted into the reactor to support the coal sample (11). The gasification
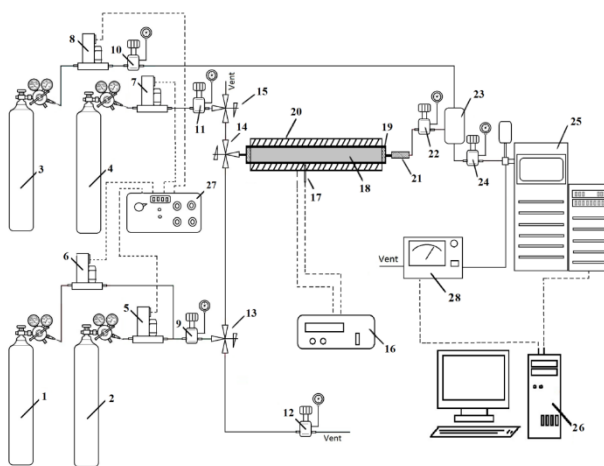
temperatures (i.e.,

G-Figure 1 Schematic diagram of catalytic coal gasification

700°C, 800°C, and 900°C) were adjusted in a tubular furnace (10, Thermolyne 21100). The tar

and water in the product gas were separated from the syngas through a water-cooled condenser

(15) and collected (22) for analysis. The pressure of the whole gasification system was regulated

by another back pressure regulator (13, GO Regulator) and monitored using pressure gauges (16,

17). The reactor was protected against overpressure by a pressure relief valve (8). Then, the

cleaned syngas passed through a desiccant-filled water trap (18) for further water removal prior to flow measurement (19). The syngas was then either vented to the fume hood or analyzed by a gas chromatograph (Agilent 3000A micro GC) (20) equipped with two micro-columns (18, MolSieve 5A PLOT and 4 m PoraPlot U) to separate H_2, CO, N_2, CO_2, and light hydrocarbons such as CH_4, prior to concentration analysis using a calibrated thermal conductivity detector (TCD). All collected data were documented using a data acquisition system (21).

2.2 Pre-combustion CO_2 separation

All experiments are conducted in the one column adsorption apparatus as shown in C-**Error! Reference source not found.**Figure 1. The apparatus was constructed with stainless steel tubes. All parts were connected with 1/8 in i.d. tubing and Swagelok three-way valves. The stainless steel adsorber has a length of 22 cm and an inner diameter of 1/2 in. The adsorber is wrapped by an electric heating tape and the temperature is monitored using a K type thermocouple. The adsorber is insulated to allow for

C-Figure 1 Schematic of high-pressure adsorption apparatus

conducting experiments at a variety of temperatures with minimum heat loss. The system pressure is preserved by Swagelok back pressure regulators (9, 10, 12, 14, 22, and 24). The mass

flow rate controllers (5, 6, 7, and 8) and the CM4 MFC Power Supply/Control Module (27) were purchased from Parker. The volume of the buffer tank is 300 cm^3. The mass spectrometer (MS, Agilent 5975C) and the H$_2$ analyzer (Horiba TCA-300) were used to monitor the outlet gas composition online. A combination of manual and automatic valves allowed for numerous options of flow. The adsorption/desorption operation is controlled through the LabVIEW software.

Prior to experiments, the MFCs, the MS, and the H$_2$ analyzer were calibrated. In the calibration process of MFC, the inlet and outlet pressures of MFC for all the gasses (H$_2$, CO$_2$, and N$_2$) were kept at 20 bar and 15 bar using corresponding pressure regulators. However, the flow
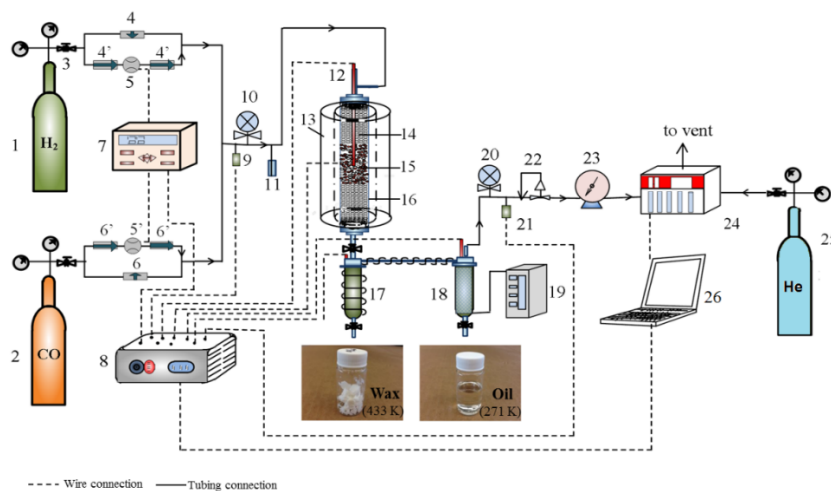rate of Ar, as the trace gas, was kept at a constant value and the inlet and outlet pressures of MFCs were kept at 80 psi and 20 psi, respectively. A regulator (24) was utilized to ensure the inlet pressure of MS was kept stable at 1.1 bar. All the MFCs were calibrated with a Wet Test Meter (Elser American Meter).

Nanoporous TiO$_2$ was mixed with sand to avoid an excessive pressure drop of the gas stream along the adsorber (16). The CO$_2$/H$_2$ mixture, with varying CO$_2$ to H$_2$ mole ratios, was fed into the adsorber using MFC (5) and MFC (6). The CO$_2$/H$_2$ separation was performed through two consecutive steps, adsorption and desorption. Adsorption started with introducing N$_2$ into the adsorber until the pressure in the adsorber elevated to a set value; followed by closing the back pressure regulator (22) and simultaneously venting the incoming N$_2$ through two 3-way valves (13 and 14). In this manner, the pressure inside the adsorber was maintained at the constant set value, while the concentration of N$_2$ entering MS gradually decreased as shown in C-**Error! Reference source not found.**Figure 2a. The flow conditions were varied as designed:

CO_2 from its cylinder (1), H_2 from its cylinder (2), or a CO_2/H_2 mixture prepared with two MFCs [H_2 MFC (5) and CO_2 MFC (6)] were introduced into the adsorber to displace the filled N_2. The gas sorption step proceeded until equilibrium concentration profiles of CO_2 and H_2 were observed on the MS, and the apparent mole decrease(s) of the gas(es) during the whole sorption period, $M_{j,a}$ was calculated. The next step required the regulator (22) to shut off the flow from the filter (21) into the buffer tank (23). The volume(s) of CO_2 or H_2 in the space from the regulator (22) and MS, $M_{j,bpr-MS}$ was then measured.

2.3 FT synthesis (FTS) for diesel production

FTS reactions were performed in a stainless fixed-bed reactor with an inner volume of 38 mL (F-Figure 1). The catalyst (3.0 g) (15) was well dispersed with quartz sand (sand size: 30-40

F-Figure 1 The schematic diagram of fixed-bed reactor (FBR) system. (1) Hydrogen cylinder; (2) Carbon monoxide cylinder; (3)(3') Pressure regulators; (4)(6) Valves; (4')(6') By-pass valve; (5) Mass flow controller; (7) CM-400/scanner; (8) Automatic controller/scanner system; (9) Front pressure sensor; (10) Front pressure gauge; (11) Safety valve; (12) Thermocouple; (13) Furnace; (14) Sand; (15) Catalyst; (16) Fixed-bed reactor; (17) Hot trap; (18) Cold trap; (19) Chiller; (20)

Backpressure gauge; (21) Back pressure sensor; (22) Back pressure regulator; (23) Wet gas flow meter; (24) Gas chromatography; (25) Carrier gas He; (26) Computer.

mesh) and loaded in the center of reactor with a thermocouple inside. Two mass flow controllers (5 and 5') were used to automatically adjust flow rate of the inlet gasses comprising CO and H_2 (high purity of 99.999 %). Mixture of CO and H_2 was subsequently introduced into the reactor which was placed inside a tubular furnace (13). Temperature was controlled by an automatic temperature controller (8) and monitored by a computer through a thermocouple (12) inserted into catalytic bed. The catalyst was in situ reduced at atmospheric pressure under H_2 at 400 °C for 10 h before the reaction started. In each test, 3.0 g catalyst was loaded and the all the date was collected after the time point of 20 h to ensure steady state operation was attained.
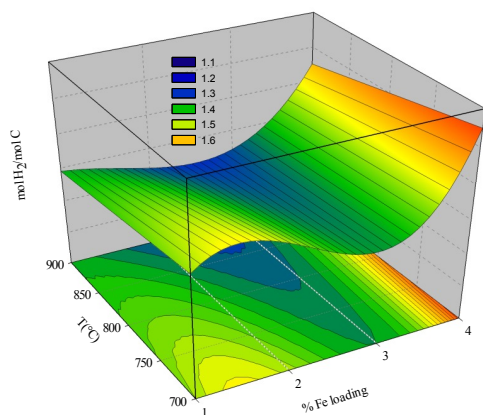
The FT reaction was carried out with the temperature of 220/240 °C, , a total pressure of 2.0 Mpa with the molar ratio of H_2 to CO of 2:1 and space velocity of 800 mL/g.cat/h. During the reaction, the synthetic wax was collected by a hot trap with temperature of 160 °C while the fluid oil was gathered by a cold trap (T = 0 °C). A pressure gauge located before the back pressure regulator (20) was used to monitor the desired pressure. The reactions parameters were controlled and recorded by LABVIEW FTS process program. After the cold trap, the tail gas was analyzed by an on-line gas chromatography (GC-8610C, SRI instruments, Inc.) equipped with thermal conductivity detector (TCD) and flame ionization detector (FID), through a molecular sieve 13x column and a 60m capillary column, respectively. The liquid products were analyzed via a different gas chromatography (GC-7890A, Agilent, Inc.). The wax phase components were dissolved in CS2 and analyzed by the Agilent GC. The reaction performance results including

CO and H_2 conversion, HCs' selectivity, yield of products and rate of HCs ($C_1^+(C_1-C_4)$ and C_5^+) were subsequently calculated.

3. RESULTS AND DISCUSSION

3.1 Gasification

G-Figure 2 shows the hydrogen molar yield (normalized per mole of carbon in the char) as a function of iron loading and pyrolysis temperature. Higher loadings of iron generally produce higher yields. Higher loadings of iron generally produce higher yields of H_2, as indicated in G-
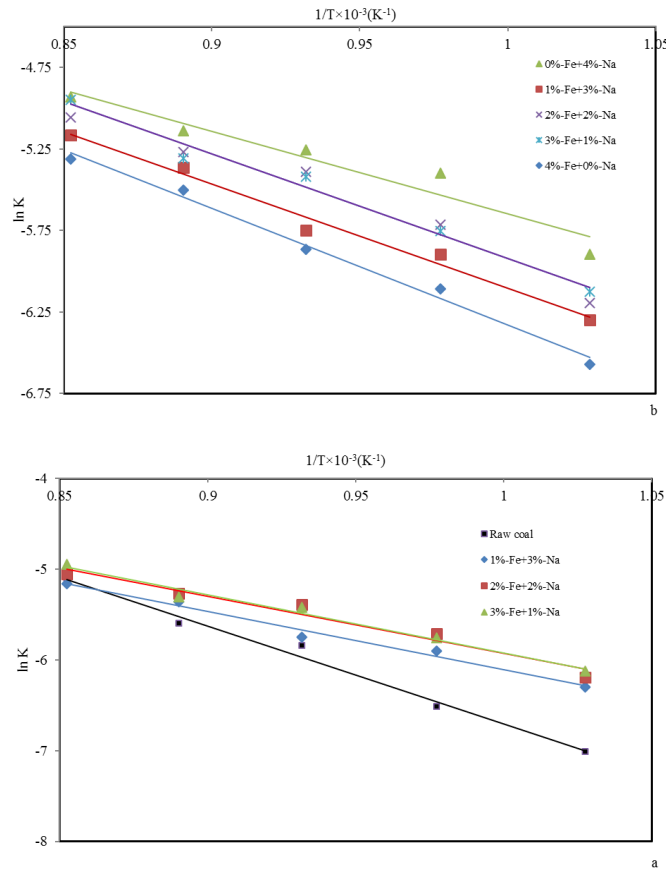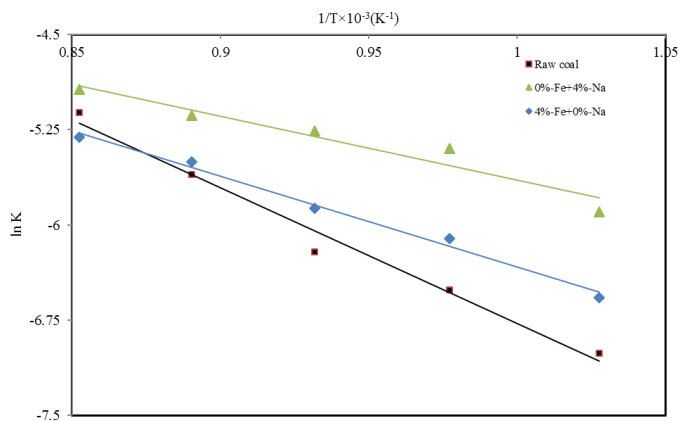

G-Figure 2 Molar yields of H2 per mole of carbon in the char vs. loadings of Fe and gasification temperatures [Numbers 1, 2, 3 and 4 in the Fe loading axis represent 1%-Fe+3%-Na, 2%-Fe+2%-Na, 3%-

Figure 2, with the exception of the 3%-Fe+1%-Na catalyst and coal mixture, which produced the least amount of hydrogen among the studied catalysts per mole of carbon in the char. This effect is apparently related to the higher rate of conversion of the 3%-Fe+1%-Na mixture compared to the other composite ones, which was also observed during pyrolysis. Much of the hydrogen formed during the gasification step was obtained from H_2O through the water-associated reactions, including the water gas shift (WGS) reaction. The coal loaded with the 4%-Fe+0%-Na catalyst produced the highest amount of hydrogen. The hydrogen production at 800°C increased

from 1.25 mol H_2/mol C with raw coal to 1.45 mol H_2/mol C with the 4%-Fe+0%-Na catalyst and coal mixture, a 16% increase.

G-Figure 3 shows the Arrhenius plots for the carbon conversions accelerated by the composite catalysts. The comparisons of carbon conversion reaction rate constants indicate that the 3%-Fe+1%-Na catalyst is better than the 2%-Fe+2%-Na and 1%-Fe+3%-Na ones. The superiority of the 3%-Fe+1%-Na catalyst when compared to the 2%-Fe+2%-Na catalyst is not fully evident in Figure 3a because during the first stage of the reaction through which the shrinking core model is applicable, the difference between these two catalysts is trivial. At high temperatures, raw coal is superior to the pure-iron catalyst (4%-Fe+0%-Na) (G-Figure 3c), which is also

G-Figure 3. Arrhenius plots: a) 3 composite catalysts and raw coal b) Iron and sodium pure catalysts and raw coal. c) Pure iron and sodium catalysts and composite catalysts.
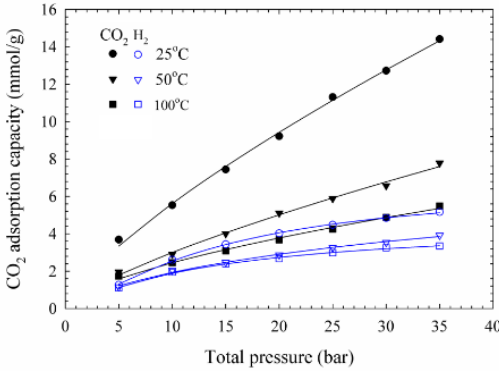
being investigated in the previously mentioned ongoing research. Cerfontain et al. [G1] stated that the rate determining step of the alkali metals based catalytic coal gasification mechanism is the decomposition of an intermediate carbon-oxygen surface species, the rate determining step is the oxygen transfer from the metal oxide species, namely Na_2O and Fe_3O_4.

A decrease in the activation energies with the use of any of the studied catalysts was observed when compared to the result exhibited by raw coal. The composite catalysts reduce the activation energy of carbon conversion by ~30-40%. The activation energy obtained with non-catalytic coal gasification was 89.0 kJ/mol, which was reduced to ~52 kJ/mol with the use of the 2%-Fe+2%-Na catalyst.

3.2 CO$_2$ separation

As shown in C-Figure 2 sorption capacities for CO_2 and H_2 decrease with increasing the temperature from 25-125°C, due to dominant physical adsorption on the surface of nanoporous TiO_2. For pure CO_2 and pure H_2 adsorption, the most widely used analytical isotherms are:

Langmuir isotherm and Freundlich isotherm. The Langmuir model describes monolayer adsorption (the adsorbed layer is one molecule in thickness) on an ideal and flat surface assuming surface homogeneity, localized adsorption on the solid surface, and energetically equivalent

C-Figure 2 Experimental and theoretical adsorption equilibrium isotherms of single component CO_2 and H_2 on TiO_2 at different temperatures [Symbols: experimental; Solid lines: theoretical].

adsorption sites [C1]. Freundlich describes the non-ideal and reversible adsorption. This empirical model can be applied to multilayer adsorption, with non-uniform distribution of adsorption heat and affinities over the heterogeneous surface. Furthermore, Sips isotherm [C2] is a combined form of Langmuir and Freundlich expressions [C2]. Sips isotherm equation can be written in the following general form:
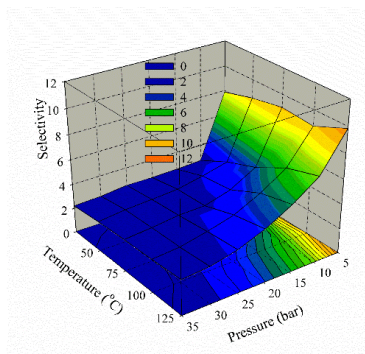
$$\frac{q}{q_e} = \frac{K \cdot p^{1/n}}{1 + K \cdot p^{1/n}} \qquad \text{(C-E1)}$$

where q and q_e are the number of moles adsorbed at a given pressure and the number of moles adsorbed at saturation, respectively, p is the pressure and n are constants. The constant n is often regarded as the heterogeneity factor, with values greater than 1 indicating a heterogeneous system. Values close to 1 indicate a material with relatively homogenous binding sites. For $n = 1$, the Sips model becomes equivalent to the Langmuir equation [C1].

Adsorption processes in porous materials are governed by the interplay between the

strength of fluid-wall and fluid-fluid interactions; as well as the effects of confined pore space on the state and thermodynamic stability of fluids confined to narrow pores. These governing interactions manifest themselves in the shape or type of the adsorption isotherm [C3]. In this study, we used the Sips isotherm to model the single-component CO_2 and H_2 adsorption data at different temperatures, as shown in C-Figure 2. The adsorbed amount of H_2 and CO_2 increased continuously while pressure increased and a gradual flattening was observed for H_2 when the pressure was sufficiently high; however, the CO_2 isotherms were almost linear. According to International Union of Pure and Applied Chemistry (IUPAC) [C4], the adsorption isotherms shown in C-Figure 2 belong to a type I isotherm class where the uptake is governed by the accessible pore volume rather than by the internal surface area
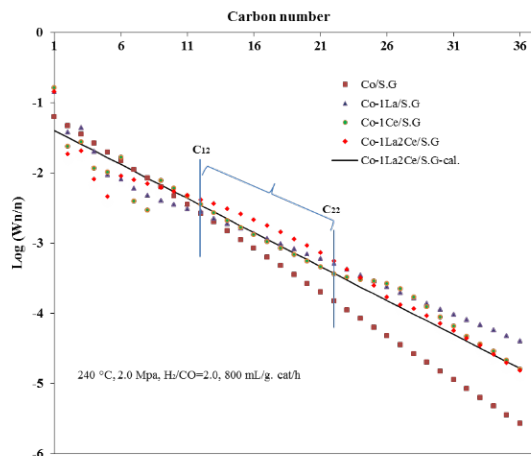
3D diagrams of TiO_2 selectivity of CO_2 over H_2 for the binary components CO_2/H_2 with molar ratio of 50/50 are shown in C-Figure 3. The selectivity of TiO_2 toward CO_2 improves as the temperature increases or the pressure decreases. The selectivity value of TiO_2 reaches 9.87 at $125^{\circ}C$ and 5 bar for CO_2/H_2 molar ratio of 50/50.

C-Figure 3 Selectivity of TiO_2 at binary-component CO_2/CH_4 with molar ratio of 50/50.

3.3   FT synthesis (FTS) to diesel

The hydrocarbon distribution, $\log(\frac{Wn}{n})$ *versus* carbon number at 240 °C, is shown in F-Figure 2. The figure shows that unpromoted catalyst Co/S.G had a lower products proportion in
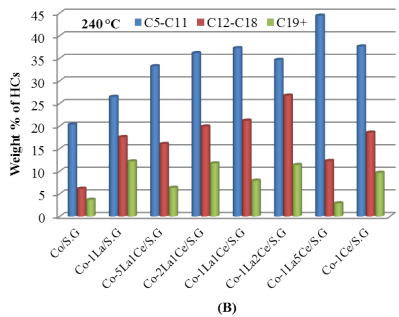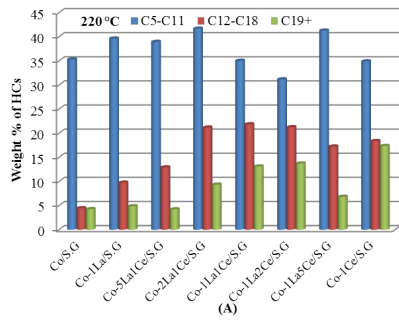
F-Figure 2. ASF plot of hydrocarbons products of selected catalysts at 240 °C.

whole distribution range while the catalysts modified with individual rare-earth (IRE) and composited rare-earth (CRE) presented higher proportion of the products with the carbon number > 12. In addition, Co-1La2Ce/S.G presented an obvious higher proportion of products (C_{12}-C_{22})

and lower proportion of long chain hydrocarbons (C_{26+}) compared with IRE promoted catalysts. It was also noticeable that, for catalyst Co-1La2Ce/S.G, C_2 came below the ASF curve, the possible explanation might be that the rate of liberation of the free C_2 hydrocarbons from the catalysts' surface was slower than the rate of C_2 polymerization which was surface-attached related [F1]. The other two points, C_4 and C_5, were also not fitted well with the curve, which might be because the vaporization of light hydrocarbon products from liquid gasoline phase during the sample collection from the high-pressure cold trap [F2].

In order to present the details of product distributions, the selectivities (weight percentage) of C_5-C_{19}^+ were listed in the F-Figure 3. In F-Figure 3A, CRE promoted catalysts showed higher

F-Figure 3. Selectivities of (C_5-C_{19}^{+}) of different catalysts at temperature 220 °C (A) and

proportion of C_{12}-C_{18} while remained the similar proportion of C_5-C_{11} (35 - 42%) compared to IRE promoted and unpromoted catalyst. The heavy hydrocarbon with n > 19 in the products was in proportion to the cerium concentration. Ce promoted catalyst achieved the highest proportion of C^{19+} (13.72%) and, among the CRE promoted catalysts, Co-1La2Ce/S.G had the highest proportion of C^{19+} (13.72%).

When temperature increased to 240 °C (F-Figure 3B), the selectivity of C_5^{+} components decreased at different levels while the productivity of C_5^{+} increased inversely due to the enhanced CO conversion. The selectivity of C_5-C_{11} increased with the increasing ratio of Ce in the CRE promoted catalysts except when the ratio of Ce to La was 1: 1. When the molar ratio of Ce to La

equaled 5:1, the highest C_5-C_{11} was achieved (44%), however, the diesel fraction rapidly dropped down to 12.28 % compared to 17.24 % at 220 °C. The highest diesel fraction (C_{12}-C_{18}) was obtained (26.77 %) when the ratio of Ce to La was 2: 1. All of the results in F-Figure 3 further

indicate that the modification of CRE facilitates the formation of diesel and gasoline fraction, which may be related to the synergistic effect of La and Ce. Overall, catalysts modified with IRE have higher selectivity of C_5^+ compared with unpromoted one at both temperatures, and the catalysts promoted with CRE had even better performances. At the appropriate molar ratios of La to Ce, such as 2:1, 1:1 and 1:2, the proportion of diesel fraction maintains at a high level at both temperatures.

4.   CONCLUSIONS

Coal gasification - The rates of carbon conversion during gasification of Wyodak PRB coal were considerably improved under different conditions by using the composite catalyst ($FeCO_3$-Na_2CO_3) when compared to those obtained from raw coal or the pure iron catalyst. The use of the composite catalyst $FeCO_3$-Na_2CO_3 during coal gasification can improve the yields of useful gasses, including hydrogen and carbon monoxide. Therefore, $FeCO_3$-Na_2CO_3 composite catalysts are promising materials for catalytic coal gasification, although more work needs to be performed before the feasibility becomes a reality.

CO₂ separation - Nanoporous TiO_2 was used for separation of CO_2/H_2 under the conditions relevant to pre-combustion CO_2 capture. Regardless of single-component or binary-component, CO_2 and H_2 adsorption capacities were improved with increasing the pressure in the range of 5-35 bar, and decreasing the temperature within the range of 25-125°C. Sips and Langmuir-Freundlich binary-component expanded isotherm adsorption (LFBE) model were used to model adsorption of pure gasses and CO_2/H_2 mixture (with the CO_2/H_2 molar ratio of 50/50) on TiO_2, respectively. The deactivation model was found to fit the CO_2 breakthrough curves well. Also, TiO_2 shows good regenerability over multiple adsorption/desorption cycles, which was confirmed by BET, XRD, and XPS analysis results. Therefore, TiO_2 is a promising cost-effective

material for CO_2/H_2 separation, although more work needs to be performed before feasibility of utilizing this sorbent becomes a reality.

Fischer-Tropsch synthesis for diesel production - Silica gel supported cobalt based FTS catalysts with SRE or MRE promoted were synthesized for producing high-value chemicals and fuels, especially diesel, through coal-derived syngas. The effects of different molar ratios of RE on the catalytic performance were studied. The synergistic effect of La_2O_3 and CeO_2 to cobalt based catalysts was found and both catalytic activity and valuable diesel fractions (C_{12} - C_{18}) selectivity were achieved with the optimized molar ratio of the RE. Meanwhile, high selectivity of C_5^+ and low productivity of methane were also achieved. XRD and TEM results showed clearly that, the catalysts modified with MRE presented lower surface area, lower pore diameter and pore volume compared to unpromoted catalyst, thus resulting in the excellent catalytic performance. The MRE promoted catalysts with optimized La and Ce molar ratio may have a potential industrial application of FTS to diesel rich synthetic oil.

5. REFERENCES

Gasification

G1.   Certofontain M, et al., Carbon 1987, 25, 351.

Pre-combustion CO_2 separation

C1.   García, S., et al., Langmuir, 2013, 29, 6042.

C2.   Foo, K. and B. Hameed, Chem Eng J., 2010, 156, 2.

C3.   Thommes, M., Chemie Ingenieur Technik, 2010, 82, 1059.

C4.   Pierotti, R. and J. Rouquerol, Pure Appl Chem, 1985, 57, 603.

FTS for diesel production

F1.   Chiusoli, G, Maitlis, P M, RSC Publishing, 2008.

F2.   Wu, B, et al., Fuel 2004, 83, 205.